

Empirical model for longwave and midwave radiometric and spatial characteristics of clouds for target detection considerations

Patrick Leslie,^{a,*} Robert Grimming^b, Sarina Grijalva,^a Steven Butrimas,^a and Ronald Driggers^a

^aUniversity of Arizona, Wyant College of Optical Sciences, Tucson, Arizona, United States

^bUniversity of Central Florida, CREOL, Orlando, Florida, United States

Abstract. The presence of clouds affects the detection of small airborne targets for infrared imaging. Clouds increase the signal of the background and create nonuniformity behind a desired target. This results in low and varying contrast. Clear sky conditions provide a low noise, uniform background that gives a better chance of detection. Understanding key variables of the clouds nonuniform structure allows for better detection and for accurate infrared search and track (IRST) models. Atmospheric modeling software, such as moderate resolution atmospheric transmission (MODTRAN), provides background path radiance in the emissive midwave infrared and longwave infrared bands. These modeled skies have been matched with measured skies in various conditions with low error. MODTRAN clouds, however, assume total cloud cover of uniform thickness and no varying transmission. MODTRAN clouds do not consider the spatially and radiometrically varying structures that make clouds unique. Studied spatial and radiometric characteristics of clouds are used in an empirical approach to predict cloud radiometric temperatures and structures with four simple equations. These cloud properties are measured at night to avoid solar contributions and focus on their emissive characteristics. The empirically modeled clouds are projections from measured or MODTRAN modeled clear skies. This method of modeling clouds allows for easy implementation of a nonclear sky background into IRST models. The range in which a target is first detected from its background can now be compared between clear and cloudy skies. © The Authors. Published by SPIE under a Creative Commons Attribution 4.0 International License. Distribution or reproduction of this work in whole or in part requires full attribution of the original publication, including its DOI. [DOI: [10.1117/1.OE.62.3.035105](https://doi.org/10.1117/1.OE.62.3.035105)]

Keywords: infrared; clouds; radiometry; longwave infrared; midwave infrared; target detection.

Paper 20221027G received Sep. 10, 2022; accepted for publication Feb. 20, 2023; published online Mar. 29, 2023.

1 Introduction

The study of the radiometric and spatial characteristic of clouds has a wide variety of applications. Clouds are used to study climate research,^{1,2} Earth-space optical communication path characterizations,³⁻⁵ radiation budget,^{6,7} atmospheric physics,^{8,9} and the prediction of future weather.¹⁰ Longwave infrared (LWIR) and midwave infrared (MWIR) thermal imagers have increased in accessibility for this research due to their inexpensive costs with good spatial and thermal resolution. The use of radiometers also allows for the study of clouds at night when reflective bands cameras (400 to 2000 nm) would not have enough light for analysis. Most current systems deployed for the list of research topics operate in the LWIR (8 to 14 μm). This emissive band offers high atmospheric transmission, high emissivity of its targets, and in general no reflections for most diffuse surfaces. A few systems utilize the MWIR (3 to 5 μm). The spectral content that is available in this emissive band can offer other information, but in terms of blackbody equivalent (BBEQ) temperature, the MWIR has higher path radiance, an order of magnitude-less thermal radiation and reflections that needed to be accounted for the daytime and the nighttime.

*Address all correspondence to Patrick Leslie, leslieps@arizona.edu

The study of cloud spatial characteristics has not been extensive. For most applications stated above, the identification of cloud versus clear sky has been the main goal.¹ The more in-depth studies include converting radiance of clouds into an optical density (OD) map for Earth-space optical communications.³ This OD map can then be used to predict the attenuation through clouds for other wavelengths. What is not specifically evaluated in these studies are the characteristics of the spatial distributions of the cloud radiometric data for how it affects the signal-to-noise ratio (SNR) in target acquisition, and the frequencies contained in their power spectral densities (PSDs). These features of clouds are studied to compare measured and modeled clouds.

The radiometric characteristics of clouds have been well documented for radiation budget research, meteorological processes, solid versus liquid water phase measurements, and the conversion of radiance to OD. Cloud top brightness temperature measurements are well studied and modeled for these same applications.¹¹ Accurate radiometric and spatial models have not been created for ground to sky cloud BBEQ temperatures. Understanding the minimum BBEQ, maximum BBEQ, variance, and transmission of clouds is important to the problem of placing clouds into the background of infrared search and track (IRST) models and simulations for target detection.

2 Background

The range in which targets can be identified with a given probability is an important performance metric for LWIR and MWIR sensors in IRST systems. IRST models are used to run scenarios that calculate the range in which an unresolved target can be first detected. These calculations consider the SNR of an image, given a specific background behind a target.¹² The importance of the model is to predict, detect, and track the signatures of real targets before they come into harm's way. This interest comes from an increase in attacks on airports,¹³ political figures,¹⁴ and military bases,¹⁵ from unmanned aerial vehicles (UAVs). These low cost, high payload drones can easily carry improvised explosives or perform surveillance in controlled areas from miles away from the operator. Even in the current conflict in the world, cheap drones are being used to drop Molotovs onto tanks.¹⁶ Having systems in place to detect these UAVs at long ranges is vital to protecting people and sensitive information.

For an IRST model to match a real scenario, the background and target must be modeled accurately. It has been shown that for a clear sky background, moderate resolution atmospheric transmission (MODTRAN) is an accurate atmospheric model for predicting background path radiance in the LWIR and MWIR.¹⁷ Using either radiosonde historic averages or importing exact day radiosonde data from a specific location,¹⁸ the measured and MODTRAN modeled background path radiance produces similar results. The error in the SNR or signal-to-clutter ration is much lower when importing radiosonde data into MODTRAN rather than using standard atmosphere models. The accurately modeled atmospheres from MOTRAN can be used as backgrounds for IRST scenarios and give realistic imaging results. Unfortunately, weather is unpredictable and having a clear sky for every encounter is not likely. The presence of clouds significantly increases the background signal behind a target, decreasing the SNR for an IRST system. In addition, clouds introduce highly varying and unpredictable contrast in comparison to a uniform clear sky background. This warrants the need to run IRST models that include radiometric and spatially correct clouds as the background to a target.

3 Cloud Characteristics

3.1 Radiometric Characteristics

The BBEQ temperature of clouds is first compared to clear sky measurements at camera viewing angles from the horizon to zenith, 0 deg to 90 deg. The BBEQ temperature measured is a radiometric quantity that corresponds to the emittance of a source in its specific band. The clear sky measurements are referred to as background path radiance, which is a term used to describe the signal behind a target of interest. Nevertheless, for both bands, the quantities are converted to BBEQ. For measurements, the LWIR radiometer is an FLIR T1020sc with a 28-deg field of view

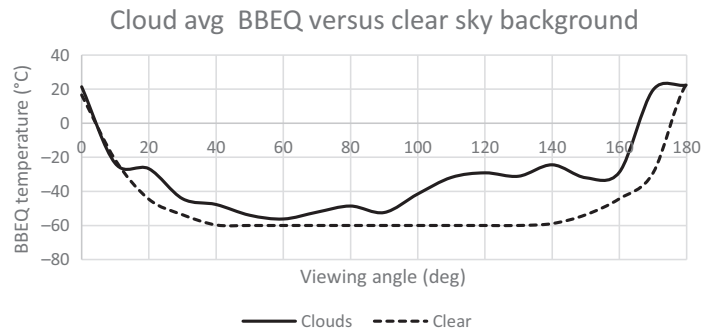


Fig. 1 The background path radiance is an uniform function that decreases as the viewing (elevation) angle increases and is constant in azimuthal scanning direction. The cloud BBEQ temperature, however, cannot be predicted based on viewing angle alone and changes in any viewing direction. One data point for cloud BBEQ temperature per viewing angle is also not enough to create simulated clouds. The clear sky data do not read below -60°C due to the limitations of the LWIR radiometer, and the slight asymmetry of the curve is due to the accuracy of the elevation angle in these first measurements.

(FOV) and the MWIR is a Telops SPARK M150 with a 21-deg FOV. Both sensors have a minimum resolvable temperature difference of 20 mK. The LWIR has a minimum BBEQ temperature limit of -60°C and the MWIR at 0°C . Most measurements in this study are performed in Tucson, Arizona, United States, but a contrasting atmosphere in Orlando, Florida, United States, is compared with the same radiometers.

The first angle that a distant drone would be detected is near the horizon, but all angles are taken into consideration. All measurements made are performed after sunset to avoid thermal contributions from the Sun in the MWIR, which provides significant solar scatter contributions. A partly cloudy sky is first measured to obtain both cloud BBEQ and clear sky BBEQ temperatures at the same time for each viewing angle. These measurements showed that the maximum cloud radiance is always higher than the background path radiance when a cloud is present in the FOV (Fig. 1). When simulating a sky, one maximum cloud BBEQ temperature data point cannot be used to create a uniform “cloud” region of the sky. The spatial distribution of BBEQ temperatures and the minimum BBEQ cloud temperatures must be considered for an IRST model where a drone is flying across the varying cloud BBEQ temperature.

The minimum BBEQ temperature of a cloud can be seen near the edges of the cloud (Fig. 2). The thickness of the cloud becomes so thin that the background path radiance of the clear sky can be considered transmitting through the edge. The minimum cloud BBEQ temperature is considered equal to the clear sky background path radiance. This assumption is based on the idea

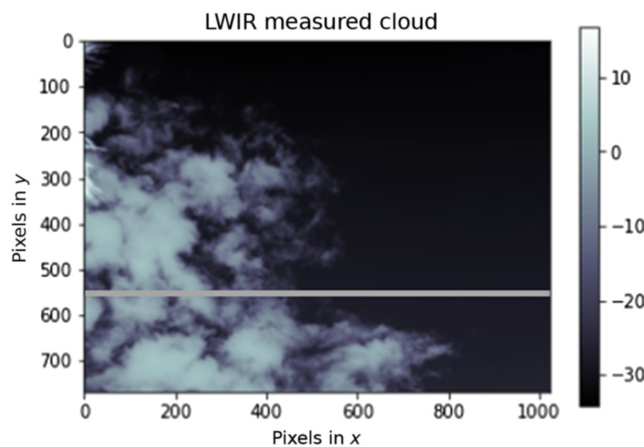


Fig. 2 Measured LWIR cloud with a BBEQ temperature cross-section cut through it. This cloud illustrates the quickly fading BBEQ temperatures toward the edge of any cloud. The transmission of the thin cloud to the background path radiance can be seen in these regions.

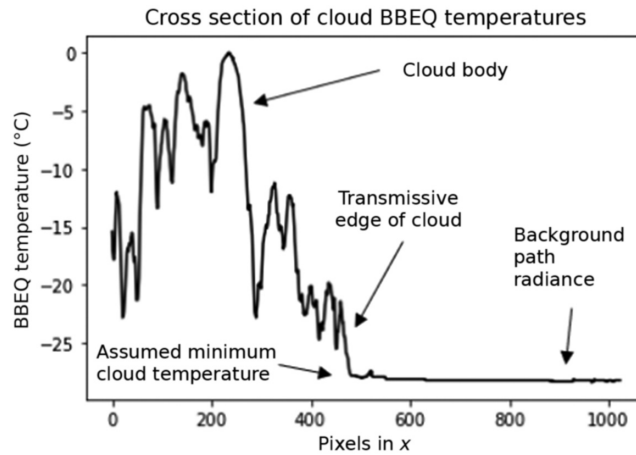


Fig. 3 Cross-sectional plot of BBEQ temperature through the cloud in Fig. 2. The cloud body bulk BBEQ temperature can be seen varying as it heads to the transmissive edge of the cloud. As the transmission of the cloud approaches 100%, the cloud minimum BBEQ temperature is assumed just before only the background path radiance is viewed.

that signal received from the transmissive cloud edge becomes 0.01% cloud BBEQ temperature signature and 99.99% clear sky BBEQ temperature. The clouds minimum BBEQ temperature essentially becomes the clear sky BBEQ temperature measured. This is seen in the cross-sectional plot of BBEQ temperature of a cloud going across the thick body and over to the sky behind it (Fig. 3). It is important to note that the thermal and spatial resolution of these transmissive edges will depend on the sensors used. With a lower operating range for the sensors, more detailed minimum temperatures could also be captured that are not in this study.

The distribution of BBEQ temperatures depends on the percent of cloud cover. The difference between the minimum and maximum BBEQ temperatures for a single cloud is much larger in the LWIR than the MWIR (Fig. 4). This is also seen in the difference between horizon and zenith background path radiance measurements for both bands.⁷ This difference is due to the higher path radiance seen in the MWIR as compared to the LWIR. However, in both bands, the histograms for BBEQ temperature tell the same story. For smaller sized clouds, the distribution of BBEQ temperatures is a small curve with all BBEQ temperatures generally equal in occurrence. As a cloud increases in percent coverage, the curve simply elongates to account for the warmer BBEQ temperatures observed in a thicker cloud body. In some cases, the ends of the histogram can raise depending on the cloud shape and the amount of cloud edge seen in the FOV of the sensor. When the cloud cover increases to total sky coverage, a cold tail is observed with a strong Gaussian-like distribution of BBEQ temperatures. These radiometric characteristics are used to help identify where cloud radiance appears relative to the background path radiance.

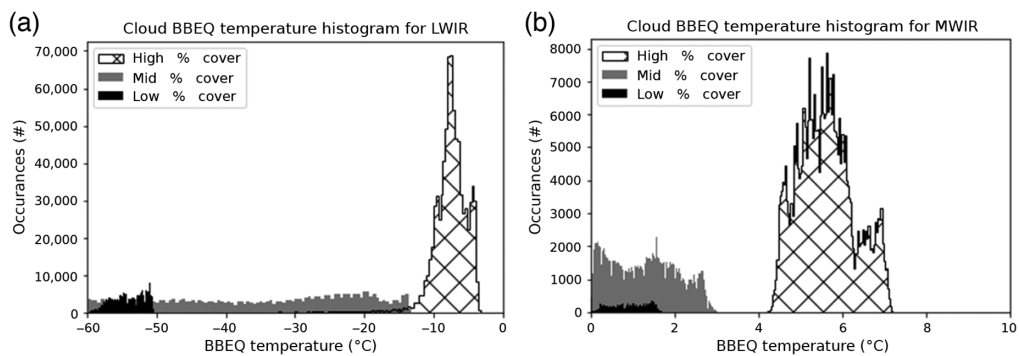


Fig. 4 Histograms to represent the spread of data for the (a) LWIR and (b) MWIR different groups of percent cloud cover. For most clouds, these three observed curves can be used for the spread of radiometric data measured.

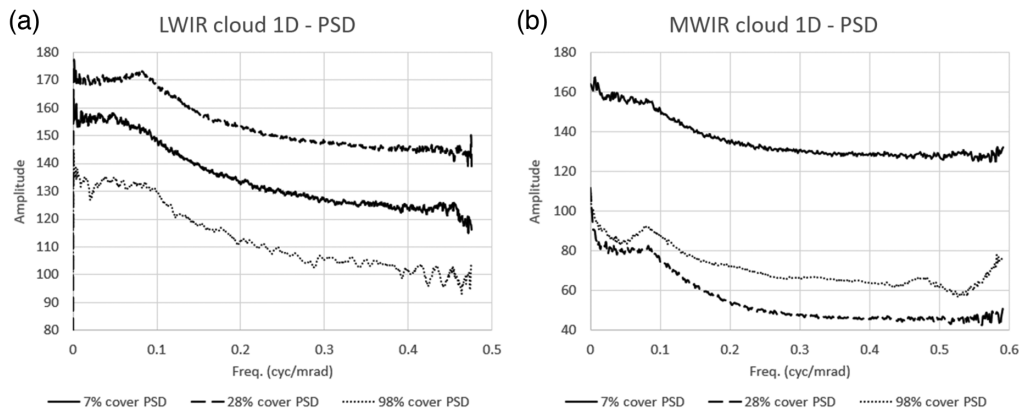


Fig. 5 PSD content for clouds of varying cover percentage. The cloud cover number stated is not measured by the percentage of clouds in the sky, but the percentage of clouds that cover the sensor as a measurement is made. The (a) LWIR and (b) MWIR clouds are the same cloud measured with different FOV's. Each measurements made was taken at a more side viewing angle of these clouds.

3.2 Spatial Characteristics

The spatial characteristics of clouds investigated are their 1D PSDs and the radiometric distribution of BBEQ temperatures within the cloud body. The 1D PSD is studied both to observe the frequency content contained in a cloud and to compare spatial distributions. Since clouds are extremely random structures, the 1D PSD can be used to categorize clouds into groups. The division of clouds that become most distinguishable is related by their percent coverage. For both LWIR and MWIR, the middle group of clouds ($\sim 25\%$ to 75% cover) shows a peak further into the frequency curve most likely due to the increased periodic structure around the edges. As the clouds increases to full cloud coverage, the PSD is almost linear and the cloud appears uniform. For small clouds, a similar shape is seen to the middle group but without the peak of periodic structure due to its small shape (Fig. 5). In the LWIR, this effect is typical, whereas in the MWIR, more content might be seen in the high-percentage cloud cover possibly due to Earth reflections. The study of the 1D PSD is important for comparing the measured and modeled cloud structure for spatial validity.

4 MODTRAN Modeling

Radiosonde data can be used to more closely match the path radiance of any atmosphere and that work inspired using the same concept for cloud BBEQ temperatures.¹⁷ Similar to the approach with the clear skies, nighttime cloud data are taken near the time of a radiosonde sounding¹⁸ so the atmospheric data matched in time. The cloud modeling was done in the MODTRAN GUI version 6.1.2. To model clouds in MODTRAN, the altitude of the clouds at the time of the measurements is also recorded using meteorological terminal air report (METAR).¹⁹ The set of data from both radiosonde and METAR reports is used to generate an atmosphere with clouds modeled in MODTRAN. The cumulus-measured cloud BBEQ temperatures are compared to the cumulus-modeled cloud BBEQ temperatures at viewing angles from 0 deg to 90 deg (Fig. 6).

The relative MODTRAN modeled cloud BBEQ temperature is far greater than the maximum measured cloud BBEQ temperatures. Although the thickness of the clouds can be changed in MODTRAN, past 1-km thickness of cloud, the BBEQ temperature does not increase substantially. The sets of data compared to MODTRAN were close to full cloud cover that results in clouds thicker than at least 500 m. Thinner than 500-m thick clouds cause the BBEQ temperature to start to drop. In this regard, the thinner clouds are identified as cloud transmission in the LWIR and MWIR. This allows us to account for the background path radiance influencing the thin or transmissive edges of the cloud.

The modeled MODTRAN cloud BBEQ temperature outputs uniform layers of radiance with no variation or transmission throughout the cloud body. This does not represent a real cloud,

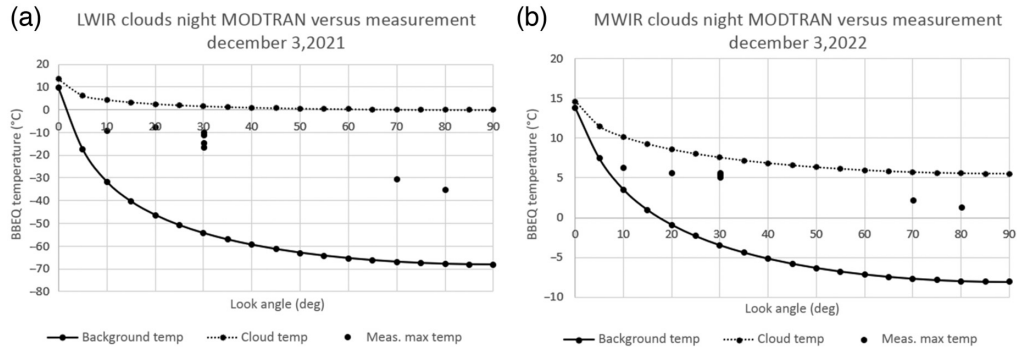


Fig. 6 Modeled MODTRAN background path radiance and modeled cloud radiance for each viewing angle. Plotted against it are measured cloud maximum BBEQ temperatures to compare the MODTRAN output. Both (a) LWIR and (b) MWIR are plotted and neither maximum BBEQ temperature approaches the MODTRAN model.

which has a lot of spatial concentration variation and no radiometric uniformity. The only way to overcome this in MODTRAN is to simulate each pixel with varying thickness, altitude, and transmission. This method becomes very tedious and takes many more inputs than the empirical method below. The cross-section of the measured cloud from Fig. 3 illustrates the variation in maximum BBEQ temperature, thickness, and transmission when comparing to the single output that MODTRAN produces. Observed is also a lot of transmission near the edges of the clouds in the LWIR and MWIR. Based on the observations with measured cloud data, the extremely high spatial variation and radiometric distributions show the need for a better model for cloud BBEQ temperature.

The effect of cloud altitude and cloud thickness on cloud BBEQ temperature is studied by modeling clouds with different altitudes and thicknesses in MODTRAN (Fig. 7). The MODTRAN modeling again used the radiosonde data method to create cloud radiometric temperatures expected in Tucson, Arizona, United States, for the month of February. Although MODTRAN does not output spatially realistic clouds as demonstrated in Fig. 6, the relative changes in radiance still provide a good description of these effects versus cloud BBEQ temperature. Like driving up a mountain where the air temperature becomes colder, the temperatures of clouds decrease as they increase in altitude. For the same thickness cloud modeled, the increase in altitude above ground level dramatically decreases the cloud body BBEQ temperatures. This effect is also observed in measured cloud data. The thickness of a cloud for a single altitude also affects the BBEQ temperature of the clouds but in a much less dramatic way. The real effect is seen along the very thin transmissive edges of the clouds below 250 m of thickness that the

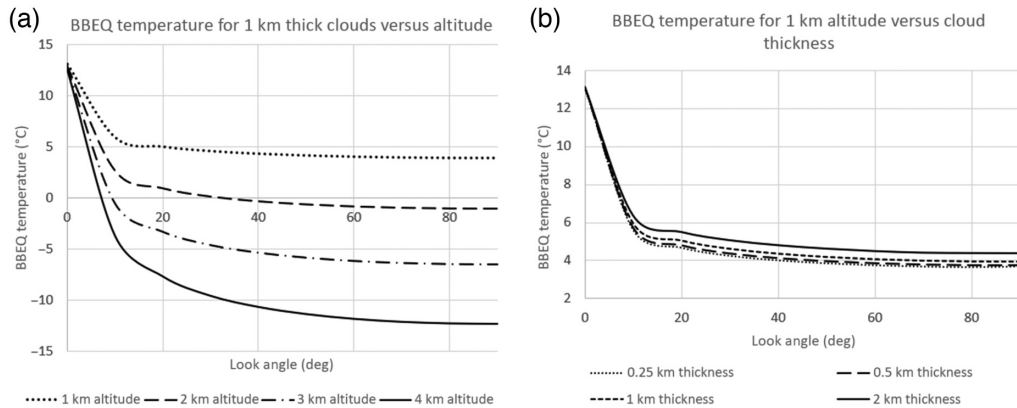


Fig. 7 (a), (b) Modeled cloud BBEQ temperature for Tucson, Arizona, United States, in February. This modeled the LWIR band, but the same effects are seen in the MWIR with their relative magnitude in changes.

500-m plus variation in thickness causes small temperature changes. This is also observed in measurements.

5 Empirical Cloud Model

The empirical cloud model is a projection of cloud BBEQ temperature from measured or modeled background path radiance measurements. The model comes from various observations in modeling and measurements. This model also provides a method for remapping existing cloud temperature distributions for the newly modeled temperatures. Measured and model-matched background path radiance in Tucson, Arizona and in Orlando, Florida, United States showed that clouds that appear in one atmosphere would not be able to be measured in the other (Fig. 8). LWIR and MWIR clouds in Tucson appear much colder relative to clouds that exist in Orlando. This means that translating the radiometric values from one cloud measured from one atmosphere to another would not be feasible. Clouds add to the observed background path radiance so the clouds observed in Orlando would have higher observed BBEQ temperature than the same cloud in a cold Tucson atmosphere. The humidity of the region increases the background path radiance in Orlando and similarly influences clouds BBEQ temperature for all viewing angles from 0 deg to 90 deg. Clouds, just like background path radiance measurements, must be considered with different atmospheres.

The empirical cloud model projects the BBEQ temperatures of clouds based on the clear sky BBEQ temperature (°C), local humidity (unitless), cloud altitude (km), and cloud viewing angle (deg). All radiometric quantities used in these equations are in BBEQ temperature (°C). The “projection” of cloud data refers to the use of atmosphere data to extrapolate the cloud BBEQ temperature from background path radiance. For either the MWIR or LWIR, three equations are used to predict the maximum cloud BBEQ temperature at any viewing angle. The first equation predicts the change in cloud maximum BBEQ temperature that will be observed from a 0-deg to 90-deg viewing angle:

$$\Delta CR = \Delta PR_{10 \text{ deg to } 90 \text{ deg}} \times (1 - H) / \epsilon_{80 \text{ deg}} \tag{1}$$

ΔCR is the change in cloud radiance from a 0-deg to 90-deg viewing angle. This value is used both to calculate cloud BBEQ temperature at the horizon and to determine the spread of cloud BBEQ temperature viewed at the horizon to straight up in the sky. The $\Delta PR_{10 \text{ deg to } 90 \text{ deg}}$ is the

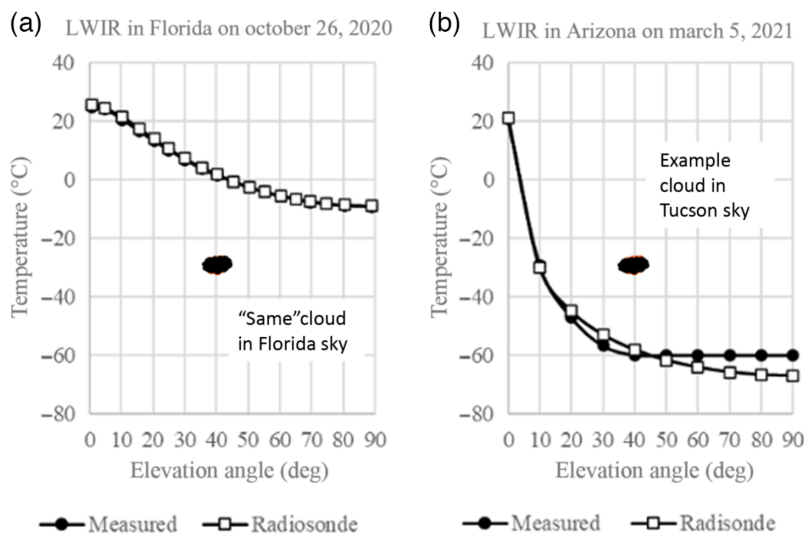


Fig. 8 Measured and MODTRAN matched background path radiance data for (a) Florida and (b) Arizona.⁷ An example cloud that could be seen in the Tucson atmosphere cannot be transferred through a simulation over to Florida without a shift in BBEQ temperature and variance. Original data obtained from Ref. 7.

change in path radiance (C) seen at a 10-deg and a 90-deg viewing angle. These values are taken from the modeled or measured background path radiance that is observed. $\Delta PR_{10 \text{ deg to } 90 \text{ deg}}$ does not consider the path radiance at the horizon $PR_{0 \text{ deg}}$ due to higher contributions from the Earth radiance and reflections. H is the humidity that is local to the path radiance observation site on the ground. $\epsilon_{80 \text{ deg}}$ is the emissivity of water at an 80-deg viewing angle in the LWIR and MWIR. This correction factor is added to account for the reflected radiance off the measured clouds due to ground radiation. In the LWIR, it is assumed that the emissivity is extremely high and $\epsilon_{80 \text{ deg}} = 1$, whereas in the MWIR the emissivity of water at an 80-deg angle is $\epsilon_{80 \text{ deg}} = 0.7$.²⁰

The following equation is used to find the cloud radiance that is observed at the horizon. This equation uses the difference in the $\Delta PR_{10 \text{ deg to } 90 \text{ deg}}$, the ΔCR just calculated, and the clouds altitude in kilometers:

$$CR_{0 \text{ deg}} = PR_{0 \text{ deg}} + |\Delta PR_{10 \text{ deg to } 90 \text{ deg}} - \Delta CR|^{(\text{Alt}_{\text{cloud}}/13)}. \quad (2)$$

The cloud altitude $\text{Alt}_{\text{cloud}}$ here is considered by raising the absolute difference of $\Delta PR_{10 \text{ deg to } 90 \text{ deg}}$ and ΔCR found in Eq. (1) to a cloud fraction. The altitude of the desired modeled clouds is divided by the maximum altitude that most clouds above sea level can form.²¹ This total value is added to $PR_{0 \text{ deg}}$, the background path radiance at the horizon, to find $CR_{0 \text{ deg}}$, the cloud BBEQ temperature that would be measured at the horizon.

To model a cloud at any other viewing angle, a sine function is used to decrease the cloud BBEQ temperature at the horizontal to zenith:

$$CR(\theta) = CR_{0 \text{ deg}} - (\sin(\theta) * \Delta CR). \quad (3)$$

This equation simply uses that the ΔCR found in the first equation, which is the difference in BBEQ temperature of a cloud found at the horizon or at zenith. The viewing angle θ is in deg. The last values needed to model a cloud are the lower BBEQ temperature bound. As seen in the spatial and radiometric characteristics of the clouds and illustrated in Fig. 3, the minimum BBEQ temperature of the clouds is bounded by the background path radiance at the cloud's viewing angle. Although this value can be used as a place holder to outline the cloud, the edge cloud BBEQ temperatures are created by a ratio of edge cloud transmission between the cloud and the clear sky BBEQ temperature:

$$CR_{\text{low}}(\theta) = \tau * PR(\theta) + (1 - \tau) * CR(\theta), \quad (4)$$

where τ is the transmission of the edge of the cloud, $PR(\theta)$ is the path radiance at that viewing angle, and $CR(\theta)$ is the maximum cloud radiance at that same viewing angle. When modeling the temperature of the cloud body and the transmission is 0, only the cloud BBEQ temperature is observed. When the transmission approaches 1, only the background path radiance is observed. This ensures when modeling the lower BBEQ temperatures of clouds and the background BBEQ temperature, the cloud is projected out of is also considered.

6 Empirical Cloud Model Results

To compare the predictions of the empirical model to calibrated sensor measurements, cloudy sky and clear sky backgrounds were measured in both Tucson, Arizona, and Orlando, Florida, United States. The same T1020sc and M150 SPARK radiometers are used to take measurements. These locations are chosen because they represent two vastly different environments for humidity and atmospheric content. The humidity ranged from 25% to 91% for a range of dates and locations. The humidity data are taken from the historically collected weather data from Weather Underground[®] or from its current weather readings of the measurement location.²² With the local humidity and METAR reported cloud altitude found for those same locations and dates, the cloud BBEQ temperatures are projected out of the measured sky BBEQ temperatures (Fig. 9). The locations and conditions are listed in Table 1. The measurements obtained in Orlando are in Fig. 9, whereas most other conditions are proved in Tucson in Fig. 10.

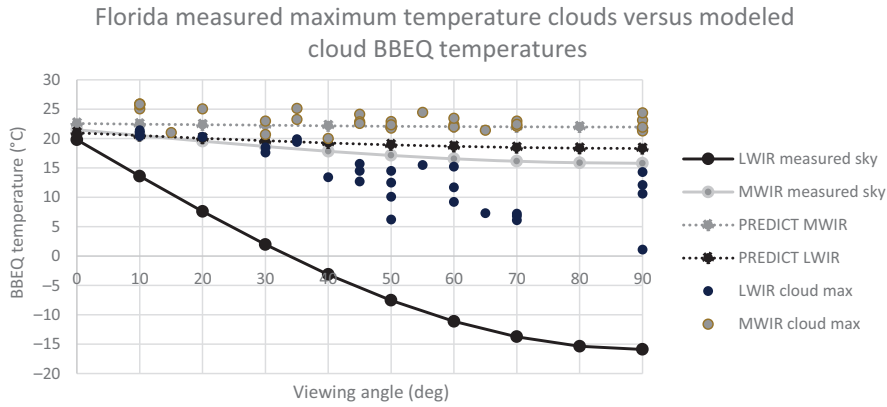


Fig. 9 MWIR and LWIR measured background path radiance with maximum cloud BBEQ temperatures plotted (scatter). Through the measured data, the empirical cloud model maximum BBEQ temperature prediction line without any added noise or variation per viewing angle (dotted).

Table 1 MWIR- and LWIR-associated empirical model parameters. Various altitudes and humidities are shown for the validation of the model.

	LWIR 2	LWIR 3	MWIR 4	MWIR 5	MWIR 6	Fig. 9
Humidity (%)	29	60	65	29	60	91
Altitude (km)	4.2	3.3	1.5	4.2	3.3	2
Location	Tucson	Tucson	Tucson	Tucson	Tucson	Orlando
Date	September 16, 2021	September 26, 2021	September 1, 2021	September 16, 2021	September 26, 2021	November 11, 2021

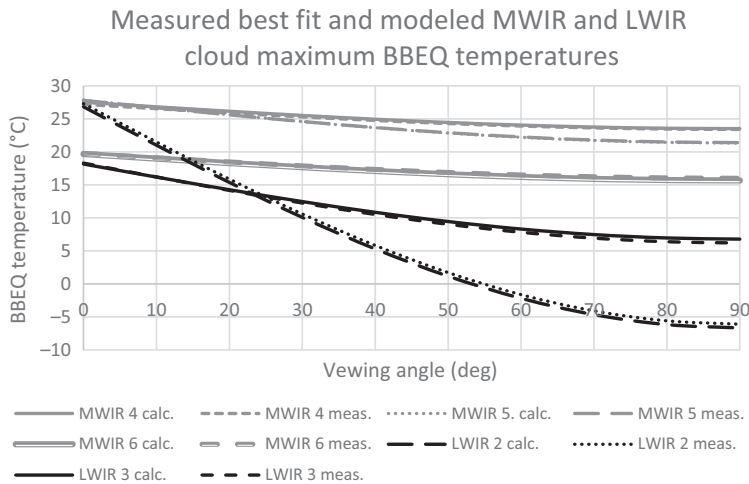


Fig. 10 MWIR and LWIR measured maximum trend in BBEQ temperature with their associated empirical model predicted BBEQ temperatures. Two LWIR and three MWIR are plotted to compare the accuracy of the equations for each band.

For Tucson and Orlando, the empirical modeled maximum BBEQ temperature predicts a reasonable match through the trendline of measured cloud maximum BBEQ temperatures for that modeled environment. The trendlines of measured and the modeled cloud maximum BBEQ temperature data are plotted for a variety of conditions (Fig. 10). This illustrates for many cases that the model matches for a variety of humidities and altitudes.

7 Discussion

The empirical cloud model equations show that the maximum and minimum BBEQ temperatures of clouds can be accurately projected from their background path radiance. With this simple method of remapping clouds, they can now be implemented into an IRST model to study the difference in range performance between clear skies and cloudy skies. To create the spatial

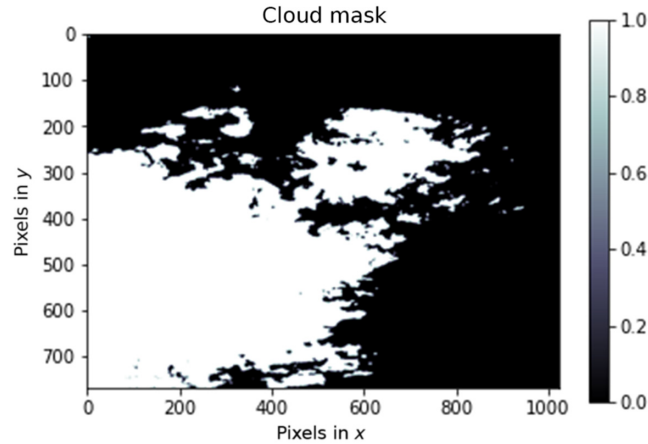


Fig. 11 The binary mask of a cloud to identify cloud pixel location in the image. Ones identify the cloud BBEQ locations and zeros identify the clear sky locations. Each individual cloud pixel is also indexed to save its spatial distribution location relative to all of the ordered cloud BBEQ temperatures.

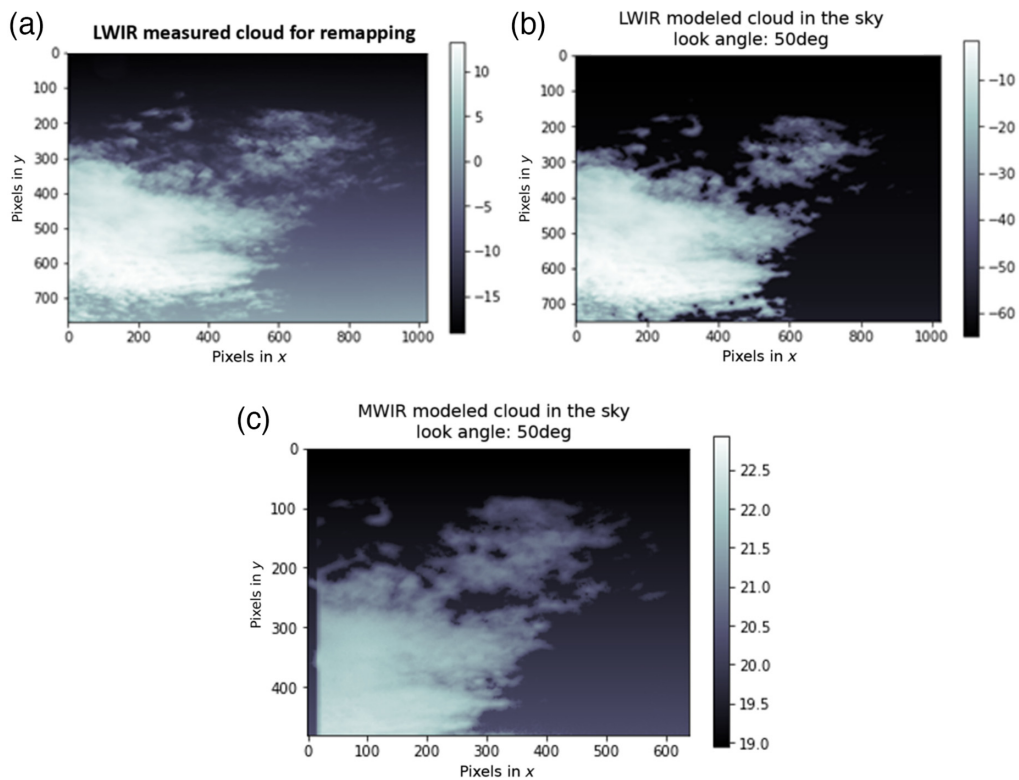


Fig. 12 (a) A cloud measured with the LWIR and MWIR radiometers at a 35-deg viewing angle. (b) An LWIR remapped cloud using the empirical equations and filling in the cloud spatial structure with the new distribution of data, in front of the modeled background sky. (c) The same cloud from the MWIR measurements is also remapped and shown to illustrate what each individual radiometers would image and simulate for the same cloud.

formation of the cloud, a previously measured cloud can be deconstructed. The identified cloud pixels in a measurement are indexed and the background path radiance is cut out of the frame (Fig. 11).

The cloud BBEQ temperatures are organized from minimum to maximum to create a distribution curve of BBEQ temperatures.²³ The empirical model then remaps the measured cloud data with the new minimum and maximum BBEQ temperatures. The distribution of the old data is scaled based on the new minimum and maximum. The new BBEQ temperature distribution is then filled into the same indexed location as its previously measured position. Finally, the transmissive edges of the clouds are taken through Eq. (4) to blend the thin cloud radiance with the background path radiance for a realistic edge profile. This method can be used to place clouds into IRST models rather than simulating their spatial structure from scratch (Fig. 12). This method is also valid for LWIR and MWIR clouds.

8 Conclusions

The method described in this paper provides for a cloud model that is radiometrically and spatially accurate. The empirical model equations take the clear sky background path radiance data and project the cloud BBEQ temperatures that can form in the sky. The comparison of modeled and measured clouds in a variety of atmospheres, altitudes, and humidities confirm the model's accuracy. Numerous static LWIR and MWIR clouds are made from this method to create backgrounds for IRST models. Future work includes creating a time evolving cloud simulation to present realistic radiometric and spatial development of clouds as a dynamic background for an IRST model. Spatial distribution of more cloud types, similar to Fig. 6, will be studied to create a more comprehensive set of spatial data. The Sun changes the cloud signatures from mostly emissive to one that contains reflections and solar loading, especially in the MWIR. All four cases, nighttime static, nighttime dynamic, daytime static, and daytime dynamic, will be studied to compare measured results to the IRST model with targets in front of cloudy sky background.

Acknowledgments

The authors would like to thank CAE Inc. for funding this work to develop their IRST capabilities. The authors declare no conflicts of interest.

Code, Data, and Materials Availability

Data will be made available upon reasonable request.

References

1. J. Shaw et al., "Cloud optical depth measured with ground-based, uncooled infrared imagers," *Proc. SPIE* **8523**, 85231D (2012).
2. B. R. Masters, "Three-dimensional microscopic tomographic imaging of the cataract in a human lens *in vivo*," *Opt. Express* **3**(9), 332–338 (1998).
3. J. Shaw et al., "Radiometric cloud imaging with an uncooled microbolometer thermal infrared camera," *Opt. Express* **13**(15), 5807 (2005).
4. P. Nugent, J. Shaw, and S. Piazzolla, "Infrared cloud imaging in support of space optical communications," *Opt. Express* **17**(10), 7862 (2009).
5. M. Partridge, "Spectra evolution during coating," figshare (2019).
6. B. Thuraiajah and J. Shaw, "Cloud statistics measured with the infrared cloud imager (ICI)," *IEEE Trans. Geosci. Remote Sens.* **43**(9), 2000–2007 (2005).
7. S. Smith and R. Toumi, "Measuring cloud cover and brightness temperature with a ground based thermal infrared camera," *J. Appl. Meteorol. Climatol.* **47**(2), 683–693 (2008).
8. J. Shaw and P. Nugent, "Physics principle in radiometric infrared imaging of clouds in the atmosphere," *Eur. J. Phys.* **34**(6), S111 (2013).

9. Y. Want et al., "Day and night clouds detection using a thermal-infrared all-sky-view camera," *Remote Sens.* **13**, 1852 (2021).
10. X. K. Shi et al., "Simulation of FY-2D infrared brightness temperature and sensitivity analysis to the errors of WRF simulated cloud variables," *Sci. China Earth Sci.* **61**, 957–972 (2018).
11. S. Proud and S. Bachmeier, "Record-low cloud temperatures associated with a tropical deep convection event," *Geophys. Res. Lett.* **48**(6), e92261 (2022).
12. R. Driggers et al., "Detection of small targets in the infrared: an infrared search and track tutorial," *Appl. Opt.* **60**, 4762–4777 (2021).
13. S. Shackle, "The mystery of the Gatwick drone," *The Guardian* (2020).
14. K. Watson, "Venezuela President Maduro survives 'drone assassination attempt'," *BBC News*, August 5, 2018 (2022).
15. M. Pomerluea, "How \$650 drones are creating problems in Iraq and Syria," C4ISRNET, January 5, 2018, <https://www.c4isrnet.com/unmanned/uas/2018/01/05/how-650-drones-are-creating-problems-in-iraq-and-syria/> (February 28, 2022).
16. H. Kesteloo, "DJI inspire 2, drones for good, Russia, Ukraine," *Drone XL*, <https://dronexl.co/2022/03/10/molotov-drone-ukrainian-military-dji-inspire/> (Accessed April 10, 2022).
17. R. Grimming et al., "Refining atmosphere profiles for aerial target detection models," *Sensors* **21**, 7067 (2021).
18. L. Oolman, "Radiosonde soundings," University of Wyoming College of Engineering <http://weather.uwyo.edu/upperair/sounding.html> (Accessed 3/9/2022).
19. G. Ballester Valor, "Metar/Speci/Taf reports selection query," *Ogimet*, <http://www.ogimet.com/metars.phtml.en> (Accessed 3/9/2022).
20. R. Branch, C. C. Chickadel, and A. T. Jessup, "Infrared emissivity of seawater and foam at large incidence angles in the 3–14 μm wavelength range," *Remote Sens. Environ.* **184**, 15–24 (2016).
21. T. Puiu, "The types of clouds: everything you need to know," *ZME Science*, <https://www.zmescience.com/science/types-of-clouds/> (Accessed 3/9/2022).
22. Weather Underground, "Historical Weather," TWC Product and Technology LLC, <https://www.wunderground.com/history> (Accessed 2/28/2022).
23. K. M. Hanson, "Introduction to Bayesian image analysis," *Proc. SPIE* **1898**, 716–731 (1993).

Patrick Leslie received his BS degree in biology from D'Youville College in 2017. He is a graduate researcher at the University of Arizona. He worked at Corning Inc. for 3 years, where he has currently earned five patents or patent applications. He began his graduate career in 2020 and his current research interests include infrared band comparisons, wide area coverage systems, and sensor system performance.

Biographies of the other authors are not available.